

Elsevier Editorial System(tm) for Pain  
Manuscript Draft

Manuscript Number: PAIN-D-09-6428R2

Title: Assessment of brain responses to innocuous and noxious electrical forepaw stimulation in mice using BOLD fMRI

Article Type: Full-Length Article

Keywords: mouse fMRI; electrical forepaw stimulation; BOLD signal; somatosensory cortex

Corresponding Author: Ms. Simone Claudia Bosshard, Dipl. Natw. ETH

Corresponding Author's Institution: Institute for Biomedical Engineering, University and ETH Zurich, Switzerland

First Author: Simone Claudia Bosshard, Dipl. Natw. ETH

Order of Authors: Simone Claudia Bosshard, Dipl. Natw. ETH; Christof Baltes, PhD; Matthias T Wyss, M.D., PhD; Matthias T Wyss, M.D., PhD; Thomas Mueggler, PhD; Bruno Weber, PhD, Professor; Markus Rudin, PhD, Professor; Markus Rudin, PhD, Professor

Abstract: Functional magnetic resonance imaging (fMRI) using the blood oxygen level dependent (BOLD) contrast was used to study sensory processing in the brain of isoflurane anesthetized mice. The use of a cryogenic surface coil in a small-animal 9.4T system provided the sensitivity required for detection and quantitative analysis of hemodynamic changes caused by neural activity in the mouse brain in response to electrical forepaw stimulation at different amplitudes. A gradient echo-echo planar imaging (GE-EPI) sequence was used to acquire five coronal brain slices of 0.5 mm thickness. BOLD signal changes were observed in primary and secondary somatosensory cortices, the thalamus and the insular cortex, important regions involved in sensory and nociceptive processing. Activation was observed consistently bilateral despite unilateral stimulation of the forepaw. The temporal BOLD profile was segregated into two signal components with different temporal characteristics. The maximum BOLD amplitude of both signal components correlated strongly with the stimulation amplitude. Analysis of the dynamic behavior of the somatosensory 'fast' BOLD component revealed a decreasing signal decay rate constant  $k_{off}$  with increasing maximum BOLD amplitude (and stimulation amplitude). This study demonstrates the feasibility of a robust BOLD fMRI protocol to study nociceptive processing in isoflurane anesthetized mice. The reliability of the method allows for detailed analysis of the temporal BOLD profile and for investigation of somatosensory and noxious signal processing in the brain, which is attractive for characterizing genetically engineered mouse models.

1  
2  
3  
4 **Abstract**  
5

6  
7  
8 Functional magnetic resonance imaging (fMRI) using the blood oxygen level dependent (BOLD)  
9  
10 contrast was used to study sensory processing in the brain of isoflurane anesthetized mice. The  
11  
12 use of a cryogenic surface coil in a small-animal 9.4T system provided the sensitivity required  
13  
14 for detection and quantitative analysis of hemodynamic changes caused by neural activity in  
15  
16 the mouse brain in response to electrical forepaw stimulation at different amplitudes. A  
17  
18 gradient echo-echo planar imaging (GE-EPI) sequence was used to acquire five coronal brain  
19  
20 slices of 0.5 mm thickness. BOLD signal changes were observed in primary and secondary  
21  
22 somatosensory cortices, the thalamus and the insular cortex, important regions involved in  
23  
24 sensory and nociceptive processing. Activation was observed consistently bilateral despite  
25  
26 unilateral stimulation of the forepaw. The temporal BOLD profile was segregated into two  
27  
28 signal components with different temporal characteristics. The maximum BOLD amplitude of  
29  
30 both signal components correlated strongly with the stimulation amplitude. Analysis of the  
31  
32 dynamic behavior of the somatosensory ‘fast’ BOLD component revealed a decreasing signal  
33  
34 decay rate constant  $k_{off}$  with increasing maximum BOLD amplitude (and stimulation amplitude).  
35  
36 This study demonstrates the feasibility of a robust BOLD fMRI protocol to study nociceptive  
37  
38 processing in isoflurane anesthetized mice. The reliability of the method allows for detailed  
39  
40 analysis of the temporal BOLD profile and for investigation of somatosensory and **noxious** signal  
41  
42 processing in the brain, which is attractive for characterizing genetically engineered mouse  
43  
44 models.  
45  
46  
47  
48  
49  
50  
51  
52  
53  
54  
55  
56  
57  
58  
59  
60  
61  
62  
63  
64  
65

1  
2  
3  
4  
5  
6  
7  
8  
9  
10  
11  
12  
13  
14  
15  
16  
17  
18  
19  
20  
21  
22  
23  
24  
25  
26  
27  
28  
29  
30  
31  
32  
33  
34  
35  
36  
37  
38  
39  
40  
41  
42  
43  
44  
45  
46  
47  
48  
49  
50  
51  
52  
53  
54  
55  
56  
57  
58  
59  
60  
61  
62  
63  
64  
65

**Title**

*Assessment of brain responses to innocuous and noxious electrical forepaw stimulation in mice using BOLD fMRI*

**Authors**

Simone C. Bosshard<sup>1</sup>, Christof Baltes<sup>1</sup>, Matthias T. Wyss<sup>2,3</sup>, Thomas Mueggler<sup>1</sup>, Bruno Weber<sup>2</sup>,  
Markus Rudin<sup>1,2</sup>

<sup>1</sup>Institute for Biomedical Engineering, University and ETH Zurich, Switzerland

<sup>2</sup>Institute of Pharmacology and Toxicology, University of Zurich, Switzerland

<sup>3</sup>PET Center, Department of Nuclear Medicine, University Hospital Zürich, Switzerland

**Correspondence:**

Prof. Dr. Markus Rudin  
Animal Imaging Center - ETH Zurich  
Wolfgang-Pauli-Str. 27  
CH-8093 Zürich  
Tel. +41 44 633 76 04 HIT E22.4  
Secr. +41 44 633 76 73 HIT E22.2  
Fax +41 44 633 11 87  
rudin@biomed.ee.ethz.ch

**Number of Text pages:** 31 pages

**Number of Figures:** 6

1  
2  
3  
4 **Abstract**  
5  
6  
7

8 Functional magnetic resonance imaging (fMRI) using the blood oxygen level dependent (BOLD)  
9  
10 contrast was used to study sensory processing in the brain of isoflurane anesthetized mice. The  
11  
12 use of a cryogenic surface coil in a small-animal 9.4T system provided the sensitivity required  
13  
14 for detection and quantitative analysis of hemodynamic changes caused by neural activity in  
15  
16 the mouse brain in response to electrical forepaw stimulation at different amplitudes. A  
17  
18 gradient echo-echo planar imaging (GE-EPI) sequence was used to acquire five coronal brain  
19  
20 slices of 0.5 mm thickness. BOLD signal changes were observed in primary and secondary  
21  
22 somatosensory cortices, the thalamus and the insular cortex, important regions involved in  
23  
24 sensory and nociceptive processing. Activation was observed consistently bilateral despite  
25  
26 unilateral stimulation of the forepaw. The temporal BOLD profile was segregated into two  
27  
28 signal components with different temporal characteristics. The maximum BOLD amplitude of  
29  
30 both signal components correlated strongly with the stimulation amplitude. Analysis of the  
31  
32 dynamic behavior of the somatosensory ‘fast’ BOLD component revealed a decreasing signal  
33  
34 decay rate constant  $k_{off}$  with increasing maximum BOLD amplitude (and stimulation amplitude).  
35  
36 This study demonstrates the feasibility of a robust BOLD fMRI protocol to study nociceptive  
37  
38 processing in isoflurane anesthetized mice. The reliability of the method allows for detailed  
39  
40 analysis of the temporal BOLD profile and for investigation of somatosensory and noxious signal  
41  
42 processing in the brain, which is attractive for characterizing genetically engineered mouse  
43  
44 models.  
45  
46  
47  
48  
49  
50  
51  
52  
53  
54  
55  
56  
57  
58  
59  
60  
61  
62  
63  
64  
65

## Introduction

Processing of noxious stimuli involves different levels and structures of the neural system. In spite of substantial progress in understanding the molecular mechanisms underlying pain, many aspects are still poorly understood. Genetically engineered mouse lines displaying altered or pathological pain states may help to elucidate the physiological and molecular basis of normal and pathological pain processing [21; 7; 17; 34]. Classically, sensory responsiveness in animals is characterized using behavior tests such as the hot plate, von Frey filaments or tail flick test [54]. These analyses, however, depend on the skills of the experimenter and require undisturbed motor function of the animal. Electrophysiological recordings of neuronal activity provide high spatial and temporal resolution. However, the method is invasive and does not allow recording signals over extended brain areas in a limited time period. An objective readout of neuronal signal processing that is non-invasive, independent of the observer performance and capable of covering the entire brain would be highly desirable. Functional magnetic resonance imaging (fMRI) has been widely used to assess changes in brain activity evoked by noxious stimuli. Noxious-evoked activation patterns revealed by fMRI correspond well with the structures of the pain processing pathway both in humans and animals [26; 11; 30; 6; 28]. There are two peripheral nerve types which process sensory input: low threshold fibers, mainly A $\beta$ , primarily mediate touch, while high threshold fibers, mainly A $\delta$  and C, conduct nociceptive signals [8]. The response to peripheral sensory or noxious stimulation in rats has been studied in depth [23-24; 39]. In contrast, only few fMRI studies in mice using electrical stimulation paradigms have been reported to date [2; 31; 33; 1]. This is mainly due to experimental challenges related with the small size of mice, putting high demands on spatial resolution and thus sensitivity.

1  
2  
3  
4 Another challenge for robust fMRI measurements in mice is the maintenance of stable  
5  
6 physiological conditions. While human fMRI experiments are carried out in awake subjects, the  
7  
8 large majority of animal fMRI studies are performed in anesthetized animals. Therefore,  
9  
10 anesthesia should neither interfere with brain activity nor act analgesic when investigating the  
11  
12 response to noxious stimulation paradigms. Unfortunately, there is no such ideal anesthetic  
13  
14 suitable for longitudinal studies e.g. for studying functional changes over time. In this work we  
15  
16 used isoflurane, the advantages of which are ease of administration and controlled dosing.  
17  
18 Despite these challenges, the development of robust mouse fMRI protocols is highly desirable  
19  
20 for investigating mechanistic aspects of signal processing under normal and pathological  
21  
22 conditions.  
23  
24

25  
26  
27  
28  
29  
30 The aim of this study was to develop a reliable stimulation paradigm to analyze the  
31  
32 somatosensory and nociceptive system in mice under isoflurane anesthesia. The high sensitivity  
33  
34 of a cryogenic surface coil enabled detailed analysis of the BOLD response in activated brain  
35  
36 regions elicited by electrical stimulation of the mouse forepaw as a function of time. BOLD  
37  
38 signal intensities were found to correlate well with the amplitudes of the electrical stimulation  
39  
40 applied. The quantitatively assessed dynamics of the temporal profile of the BOLD response  
41  
42 yielded further insight into the hemodynamic response to electrical stimulation.  
43  
44  
45  
46  
47  
48  
49  
50  
51  
52

## 53 **Materials and Methods**

### 54 *Animal preparation*

55  
56  
57  
58  
59  
60  
61  
62  
63  
64  
65

1  
2  
3  
4 All experiments were performed in accordance to the Swiss law of animal protection. 15 female  
5  
6 C57Bl/6 mice weighting  $22 \pm 3$  g were anesthetized with Isoflurane (induction 2-3 %,   
7  
8 maintenance 1.2 % in a 70 % air – 30 % oxygen mixture; Abbott, Cham, Switzerland),  
9  
10 endotracheally intubated and mechanically ventilated throughout the entire experiment to  
11  
12 ensure stable physiology (90 breaths/minute, respiration cycle: 25 % inhalation, 75 %  
13  
14 exhalation; Maraltec, Alfos Electronics, Biel-Benken, Switzerland). Animals were paralyzed by  
15  
16 intravenous (i.v.) administration of a neuromuscular blocking agent (Pancuronium bromide, 1.0  
17  
18 – 1.5 mg/kg; Sigma-Aldrich, Steinheim, Germany), which avoided interference by spontaneous  
19  
20 breathing and prevented movement artifacts during the fMRI experiments despite the low  
21  
22 isoflurane levels. A rectal temperature probe (MLT415, AD Instruments, Spechbach, Germany)  
23  
24 was inserted to keep the animal at  $36.5 \pm 0.5$  °C. Body temperature was maintained using a  
25  
26 warm-water circuit integrated into the animal support (Bruker BioSpin AG, Fällanden,  
27  
28 Switzerland). A transcutaneous electrode (TCM4, Radiometer, Copenhagen, Denmark) was  
29  
30 placed on the shaved upper hind limb of the mouse to measure blood gas levels ( $pCO_2$ ). In  
31  
32 some animals, heart rate and blood oxygenation was monitored using a MR-compatible  
33  
34 infrared sensor (MouseOx<sup>®</sup> Pulse Oximeter, Starr Life Sciences, Oakmont, PA, USA). For  
35  
36 accurate and reproducible positioning, the head of the animals was fixed with stereotactic ear  
37  
38 bars and eye cream was applied to prevent the eyes from becoming dry. For the electrical  
39  
40 stimulation a pair of needle electrodes (Genuine Grass instruments, West Warwick, USA) was  
41  
42 inserted subcutaneously into the distal and proximal end of the palm of each forepaw with a  
43  
44 distance of 2-3 mm between the two needles. The identical setup and parameters (1.5 mA)  
45  
46 were used to stimulate the hind paw of four animals.  
47  
48  
49  
50  
51  
52  
53  
54  
55  
56  
57  
58  
59  
60  
61  
62  
63  
64  
65

1  
2  
3  
4 The entire experiment lasted approximately 2 hours, of which 20 min were used for  
5  
6 preparation of the mouse, and the remaining time was used for acquiring fMRI data. The mice  
7  
8 were anesthetized throughout the duration of the experiment. Animals were used for more  
9  
10 than one experiment.  
11  
12  
13  
14  
15  
16  
17  
18

### 19 *MRI equipment and sequences*

20  
21  
22 All MRI experiments were performed on a Bruker BioSpec 94/30 small animal MR system  
23  
24 (Bruker BioSpin MRI, Ettlingen, Germany) operating at 400 MHz (9.4 Tesla). For signal  
25  
26 transmission and reception a commercially available cryogenic quadrature RF surface probe  
27  
28 (CryoProbe), consisting of a cylinder segment (180° coverage, radius = 10 mm) and operating at  
29  
30 a temperature of 30 K was used (Bruker BioSpin AG, Fällanden, Switzerland) (for detailed  
31  
32 information see [3]). The ceramic outer surface of the coil touching the mouse head was kept at  
33  
34 30 °C using a temperature controlled heating device.  
35  
36  
37  
38  
39  
40

41 Anatomical reference images in coronal and sagittal directions (slice orientations are given  
42  
43 using the nomenclature of the mouse brain atlas [13]) were acquired using a spin echo (Turbo-  
44  
45 RARE) sequence with the following parameters: field-of-view (FOV) = 20 x 20 mm<sup>2</sup>, matrix  
46  
47 dimension (MD) = 200 x 200, slice thickness (STH) = 0.5 mm, interslice distance (ISD) = 1.0 mm,  
48  
49 repetition delay  $T_R$  = 3500 ms, echo delay  $T_E$  = 13 ms, effective echo time  $T_{E,eff}$  = 39 ms, RARE  
50  
51 factor (number of echoes sampled for each excitation) = 32, and number of averages (NA) = 1.  
52  
53  
54  
55  
56  
57 Subsequently, the slices for the fMRI experiment were planned on the anatomical reference  
58  
59  
60  
61  
62  
63  
64  
65



1  
2  
3  
4 image and BOLD fMRI data were acquired using a gradient-echo echo planar imaging (GE-EPI)  
5  
6  
7 sequence with the following parameters: Five coronal slices covering a range of 2 to 5 mm  
8  
9  
10 anterior to the interaural line were recorded with FOV = 23.7 x 12.0 mm<sup>2</sup>, MD = 90 x 60  
11  
12 (acquisition) and 128 x 64 (reconstruction) yielding an in-plane resolution of 200 x 200 μm<sup>2</sup>, STH  
13  
14 = 0.5 mm, ISD = 0.7 mm, T<sub>R</sub> = 2500 ms, T<sub>E</sub> = 8.5 ms, and NA = 3 resulting in an image acquisition  
15  
16  
17 time of 7.5 seconds. The individual sections comprised the forelimb and hind limb areas of the  
18  
19  
20 somatosensory and insular cortices, and the thalamus [13]. An fMRI experiment consisted of  
21  
22  
23 112 repetitions and lasted 14 min, except for the group of 2.0 mA, where the acquisition  
24  
25  
26 consisted of 96 repetitions and lasted 12 min.

### 31 32 *Electrical stimulation paradigm*

33  
34  
35 Electrical pulses of 0.5 ms duration at a frequency of 3 Hz were applied. Current amplitudes  
36  
37  
38 were 0.5 mA (n = 8 animals), 1.0 mA (n = 8), 1.5 mA (n = 7), and 2.0 mA (n = 8) [42]. The  
39  
40  
41 stimulus strength is determined by the local current density (electric current per unit area of  
42  
43  
44 cross section), which itself depends on the placement of the electrodes. Current thresholds for  
45  
46  
47 noxious stimulation were estimated from an experiment on the hairy skin of the wrist of a  
48  
49  
50 volunteer with analogous electrode placement as in mice (distance between electrodes).  
51  
52  
53 Stimulation amplitudes of 1.5 and 2.0 mA were experienced as being **painful**, while the  
54  
55  
56 amplitude of 0.5 mA was clearly innocuous. Although innervation of human and mouse skin  
57  
58  
59 may differ, a noxious threshold in the range of stimulation amplitude of 1.0 mA appears  
60  
61  
62 reasonable.

1  
2  
3  
4 The stimulation paradigm consisted of a block design starting with a resting period of 120  
5  
6 seconds (baseline) followed by 60 seconds of stimulation. This series was repeated four times  
7  
8 and fMRI data recording was continued for another 120 seconds after the last stimulation  
9  
10 block. The duration between positioning of the mouse in the magnet bore and the beginning of  
11  
12 the electrical stimulation and fMRI recording was kept constant at 40 minutes to ensure the  
13  
14 same anesthesia conditions for all animals. This time was used for adjustment of MRI conditions  
15  
16 as well as anatomical reference and high resolution scans. Stimulation started with the left paw  
17  
18 in all animals. Following an 8 minute resting interval, the right paw was stimulated. These two  
19  
20 stimulation cycles were followed by a control acquisition without electrical stimulation.  
21  
22  
23  
24  
25  
26  
27  
28  
29  
30

### 31 32 *Data analysis*

33  
34  
35 Four regions of the brain were evaluated in detail, including the somatosensory cortex S1  
36  
37 contralateral and ipsilateral to the stimulated paw, the thalamus and a control region at the  
38  
39 ventral pallidum, a structure involved in neither the sensory nor the nociceptive pathway. In  
40  
41 addition, we looked at the S2, insular and piriform cortex in the 1.5 mA group. Statistical t-maps  
42  
43 were calculated using the general linear model (GLM) tool integrated in the Biomap software  
44  
45 program (M. Rausch, Novartis, Switzerland). GLM assesses correlations on a pixel-by-pixel basis  
46  
47 between the fMRI signal train and the stimulation paradigm. Activation was detected using a  
48  
49 statistical threshold of  $p = 0.0001$  for all experiments. With a minimal cluster size of 15 voxels,  
50  
51 two coronal sections were analyzed, of which one slice covered the thalamus, the secondary  
52  
53 somatosensory (S2) and insular cortex (IC) (2.8 mm anterior to the interaural line (IAL +2.8  
54  
55  
56  
57  
58  
59  
60  
61  
62  
63  
64  
65

1  
2  
3  
4 mm)) and the other covered the forepaw areas of the primary somatosensory cortex (S1) (IAL  
5 +3.7 mm). The respective regions-of-interests (ROIs) derived from the GLM analysis were used  
6  
7 to extract BOLD signal changes as a function of time. In cases for which the correlation analysis  
8  
9 revealed no activated voxels at the expected locations as well as for the unstimulated scans  
10  
11 ROIs were transferred from the mouse brain atlas [13]. For group analysis, EPI images covering  
12  
13 the S1 area (IAL +3.7 mm) and the thalamus (IAL +2.8 mm) were normalized to the coordinate  
14  
15 system of the mouse brain atlas [13]. The fMRI coordinates were defined as followed: the origin  
16  
17 of the right-hand coordinate system was chosen at the ventral end of the brain midline through  
18  
19 the coronal sections. The second reference point was the dorsal end of the same midline, while  
20  
21 the third point was placed on the edge of the right hemisphere at its widest point. The  
22  
23 coordinate axes were defined along the midline (y-axis) and perpendicular to it (x-axis). The  
24  
25 axes were then scaled to fit the dimensions of the mouse brain atlas, using an IDL-based  
26  
27 software developed in-house [48].  
28  
29  
30  
31  
32  
33  
34  
35  
36  
37  
38

39 For a detailed analysis of the fMRI time curve, the resulting BOLD profile was segregated into  
40  
41 two components *S* ('slow') and *F* ('fast'). Component *S* was extracted by fitting the 8 data points  
42  
43 before stimulation onset (light gray bars, shown in Fig. 3a, b) to a gamma-variate function:  
44  
45  $y(t) = a \cdot t^r \cdot \exp(-k \cdot t)$  with *a* (amplitude factor), *r* (power of growth curve), *k* (rate of  
46  
47 exponential decay) being the parameters to be optimized, while *t* is measured with regard to  
48  
49 the start of the first stimulation period (*t* = 0). The best fit curve (solid line, Fig. 3b) was then  
50  
51 subtracted from the original data to yield component *F* of the fMRI signal (Fig. 3c). The maximal  
52  
53 amplitudes of the fitted curve for component *S* and of the extracted curve for the first  
54  
55  
56  
57  
58  
59  
60  
61  
62  
63  
64  
65

1  
2  
3  
4 stimulation period of component  $F$  (see Fig. 3) was analyzed as a function of the stimulation  
5  
6 amplitude. The quantitative analysis was carried out for all ROIs.  
7  
8

9  
10 We furthermore analyzed the rates of BOLD signal increase and decay for both the first  
11  
12 stimulation cycle and the entire stimulation period. The data points of the signal decay at the  
13  
14 end of the stimulation interval (indicated by the dotted line in Fig. 5a) were used to calculate a  
15  
16 decay constant  $k_{off}$  assuming a single exponential decay function,  $S(t) = S(t = 0) \cdot$   
17  
18  $\exp(-k_{off} \cdot t)$ , with  $S(t)$  indicating the signal amplitude during the decay at time  $t$ , and  
19  
20  $S(t = 0)$  the amplitude at the end of the stimulation period ( $t = 0$ ). A minimum of four data  
21  
22 points of the decay curve with an amplitude exceeding noise levels were required for each  
23  
24 individual signal curve to allow for fitting. The BOLD signal decay rate constant was then  
25  
26 correlated to the maximum BOLD response  $S_{max}$  of the single animals (Fig. 5c).  
27  
28  
29  
30  
31  
32

33  
34 The constant  $k_{on}$  describing the initial build-up of the signal at the beginning of the stimulation  
35  
36 to its maximum was calculated assuming the following relation:  $S(t) = S_{max} \cdot [1 - \exp(-k_{on} \cdot$   
37  
38  $t/S_{max})]$  for which the initial slope yields  $(dS(t)/dt)_{t=0} = k_{on}$ , i.e. the initial slope was  
39  
40 assumed to be independent of the maximum BOLD signal.  
41  
42  
43  
44  
45  
46  
47  
48

#### 49 *Autoradiography and intrinsic optical imaging*

50  
51  
52  
53 Autoradiography with [ $^{18}\text{F}$ ]-2-fluoro-2-deoxyglucose ( $^{18}\text{F}$ -FDG) was performed on two female  
54  
55 C57Bl/6 mice according to published protocols [44; 55]. The left forepaw was electrically  
56  
57 stimulated at 1.5 mA using the parameters described above. A 5 minute stimulation period was  
58  
59

1  
2  
3  
4 followed by a one minute break. This was repeated for the entire time course of 45 minutes,  
5  
6  
7 before the animals were sacrificed and the brain extracted.  
8  
9

10 One mouse was used for intrinsic optical imaging. Reflectance from 570 nm light was measured  
11  
12 through the exposed skull using a CCD camera. The left forepaw was stimulated with a 10  
13  
14 second pulse train of 0.5 msec pulses of 1.0 mA current amplitude at 3 Hz. These experiments  
15  
16 were carried out under 1.5% isoflurane anesthesia.  
17  
18  
19  
20  
21  
22  
23  
24

## 25 **Results**

### 26 *Animal physiology and anesthesia*

27  
28  
29  
30  
31  
32 Non-invasive monitoring of the mice showed stable physiology throughout the duration of the  
33  
34 experiments. Blood gas levels of pCO<sub>2</sub> measured transcutaneously were in the range of 40 ± 10  
35  
36 mm Hg, which indicates a well adjusted ventilation of the animals [50]. Body temperature was  
37  
38 kept stable at 36.5 ± 0.5 °C for the entire experiment. The monitored heart rate was stable  
39  
40 around 500 beats per minute in all animals and no changes were detected during the  
41  
42 stimulation. After completion of the fMRI investigation, the animals recovered fast and could  
43  
44 be used for further experiments, an important prerequisite for longitudinal studies.  
45  
46  
47  
48  
49  
50  
51  
52  
53

### 54 *Signal and image quality*

1  
2  
3  
4 By exploiting the significant gain in sensitivity provided by the use of a cryogenic RF surface coil  
5  
6 for signal detection [35; 3] BOLD fMRI data sets of high quality suitable for reproducible  
7  
8 quantitative analysis have been obtained. Comparing the CryoProbe with a conventional room  
9  
10 temperature coil of similar dimensions (for detailed information on the coils see [3]) using the  
11  
12 GE-EPI sequence, a gain in image signal-to-noise ratio (SNR) of a factor of  $3.1 \pm 0.7$  (mean  $\pm$   
13  
14 standard deviation, unpublished data) was achieved. Using a coronal slice orientation proved  
15  
16 advantageous as cross-sectional images recorded  $\geq 3$  mm anterior to the interaural line were  
17  
18 largely devoid of geometrical distortions caused by local magnetic field inhomogeneities due to  
19  
20 different magnetic susceptibilities of adjacent tissue compartments. In caudal brain structures,  
21  
22 significant susceptibility artifacts have been observed due to the proximity of the air filled ear  
23  
24 cavities. This also impaired the quality of images recorded in horizontal plane view, which  
25  
26 would allow covering larger brain areas. Distortions caused by differences in susceptibility are  
27  
28 experienced on an absolute scale, i.e. they affect more extended brain regions in mice than in  
29  
30 rats due to the smaller dimensions of the mouse.  
31  
32

33  
34  
35 fMRI data showed good reproducibility (e.g. see error bars in Figs. 1 g, h) and allowed for  
36  
37 assessing differences in the BOLD response during stimulation at different amplitudes.  
38  
39  
40  
41  
42  
43  
44  
45  
46  
47  
48  
49  
50  
51  
52  
53

54 *Spatial distribution and intensity of the BOLD response*  
55  
56  
57  
58  
59  
60  
61  
62  
63  
64  
65

1  
2  
3  
4 The spatial distribution of the activated areas after forepaw stimulation at 1.5 mA (threshold  
5  
6  
7  $p=0.0001$ , cluster size: 15 voxels) for one representative animal is shown in Figure 1. The  
8  
9  
10 position of five coronal slices is indicated in the sagittal section shown in Figure 1a. Besides the  
11  
12 forepaw S1 region activated areas are present in other S1 areas (Fig. 1c-f), the primary motor  
13  
14 cortex (Fig. 1c-f), and several nuclei of the thalamus, including the ventral posterior nucleus  
15  
16 which relays somatosensory information to the cortex (Fig. 1f) [13]. Figure 1i shows the  
17  
18 distinction of the forepaw area (blue) and the hind paw area (red) after the respective  
19  
20 stimulation as an activation map of two representative animals. As expected, hind paw  
21  
22 somatosensory S1 areas were located median to the respective forepaw regions. The activated  
23  
24 cluster at the brain midline reflects signal contributions from the sagittal sinus. **No consistent**  
25  
26 **deactivations were detected in any region of the brain.**  
27  
28  
29  
30  
31  
32

33  
34 Figure 2 shows statistical maps (threshold  $p=0.0001$ , cluster size: 15 voxels) depicted on the  
35  
36 mouse brain atlas ([13], Fig. 2 a-f: IAL +3.7 mm, Fig. 2 g-l: IAL +2.8 mm) obtained from all  
37  
38 animals at different stimulation amplitudes ((a, g) 0.5 mA, (b, h) 1.0 mA, (c, i) 1.5 mA, (d, j) 2.0  
39  
40 mA). The activated clusters of individual animals were overlaid, i.e. the intensity in the  
41  
42 activation map corresponds to the number of animals displaying a significant BOLD signal (left  
43  
44 and right forepaw for each animal). Activation in response to the forepaw stimulation appears  
45  
46 in the somatosensory S1 and S2 cortices, in the thalamus and at higher amplitudes in the  
47  
48 insular cortex (regions indicated in Fig. 2e, k). For all activated regions, the spatial extent of  
49  
50 BOLD response exceeded the topological area defined on the basis the mouse brain atlas [13].  
51  
52  
53  
54  
55  
56  
57  
58  
59  
60  
61  
62  
63  
64  
65

1  
2  
3  
4 This is attributed to the fact that fMRI assesses the hemodynamic response elicited by neural  
5 activity and not the neural activity per se.  
6  
7  
8  
9

### 10 *BOLD signal changes in correlation to the forepaw stimulation paradigm*

11  
12  
13  
14  
15  
16  
17 The maximal BOLD signal intensity increased with increasing stimulation amplitude in all  
18 analyzed regions involved in sensory and nociceptive processing in a comparable manner as in  
19 the regions shown in Figures 3 and 4. Stimulation at the lowest amplitude of 0.5 mA led to a  
20 maximal BOLD signal of  $0.93 \pm 0.25$  % (in % of baseline intensity) in the primary somatosensory  
21 cortex contralateral to the stimulated paw. For amplitudes of 1.0, 1.5, 2.0 mA, the maximal  
22 BOLD signal changes in this region amounted to  $1.94 \pm 0.20$  %,  $2.54 \pm 0.22$  %, and  $3.52 \pm 0.41$  %,   
23 respectively (Fig. 3a). The maximum BOLD amplitude decreased for subsequent stimulation  
24 periods. Interestingly, the signal did not return to the initial baseline level within the two  
25 minutes resting interval following a stimulation episode, but stayed elevated until the start of  
26 the next stimulation block. The BOLD response to unilateral forepaw stimulation appeared  
27 consistently bilateral in all activated regions, including the S1 (Fig. 1, 4), thalamus, S2 and  
28 insular cortex (for 1.5 mA: Fig. 1h). The maximal BOLD signal amplitude in the regions of the S2  
29 somatosensory and insular cortex was significantly lower as compared to the S1 area. This was  
30 observed at all stimulation amplitudes except at 0.5 mA, where the amplitudes for S1 and S2  
31 area reached similar values (data not shown). There was no delay between ipsi- and  
32 contralateral responses within the time scale of the fMRI experiment (7.5 s temporal  
33 resolution).  
34  
35  
36  
37  
38  
39  
40  
41  
42  
43  
44  
45  
46  
47  
48  
49  
50  
51  
52  
53  
54  
55  
56  
57  
58  
59  
60  
61  
62  
63  
64  
65



1  
2  
3  
4 The control region, which was located in the ventral pallidum, a structure not involved in  
5 sensory or nociceptive processing, showed no change in BOLD intensity for stimulation  
6 amplitudes  $\leq 1.5$  mA (Fig. 1g, 1.5 mA). At 2.0 mA a maximum signal increase of  $0.81 \pm 0.12$  %  
7 was detected. This unspecific increase in the BOLD signal was observed in large parts of the  
8 brain. A second, cortical control region located in the piriform cortex, behaved comparable to  
9 the ventral pallidum (for 1.5 mA: Fig. 1h). No region-specific activation whatsoever, but only  
10 background noise was revealed by the analysis of the control fMRI data sets acquired without  
11 stimulation, indicating the stability of the fMRI setup including the physiological preparation  
12 (data not shown).  
13  
14  
15  
16  
17  
18  
19  
20  
21  
22  
23  
24  
25  
26  
27  
28  
29  
30  
31

### *Amplitudes of the two signal components S and F as a function of the stimulation amplitude*

32  
33  
34

35 The temporal profile of the BOLD response has been segregated into the two signal  
36 components *S* and *F* by fitting component *S* to a gamma-variate function and subtracting the  
37 best fit from the experimental data (Fig. 3b, c). Analysis of the maximal amplitude of both  
38 components for the two S1 regions and the thalamus were found to correlate with the  
39 stimulation amplitude. Linear regression analysis yielded correlation factors for component *S*  
40 (Fig. 5a) of  $R^2 = 0.98$  for the contralateral,  $R^2 = 0.97$  for the ipsilateral somatosensory cortex and  
41  $R^2 = 0.81$  for the thalamus, respectively. The values for component *F* (Fig. 5b) were  $R^2 = 0.97$  for  
42 contralateral S1,  $R^2 = 0.98$  for ipsilateral S1 and  $R^2 = 0.87$  for thalamus.  
43  
44  
45  
46  
47  
48  
49  
50  
51  
52  
53  
54  
55  
56  
57  
58  
59  
60  
61  
62  
63  
64  
65

#### Analysis of the signal dynamics of component *F*

Not only the amplitude but also the dynamic behavior of the BOLD response depended on the stimulation amplitude as demonstrated by the averaged temporal profile of component *F* of the first stimulation period of each animal (Fig. 5a). The maximum values for the S1 region contralateral to the stimulated paw were:  $1.19 \pm 0.48$  %,  $1.69 \pm 0.21$  %,  $2.47 \pm 0.18$  %, and  $2.81 \pm 0.37$  % for 0.5, 1.0, 1.5, and 2.0 mA, respectively. A striking feature of the observed BOLD response (Fig. 3c, 5a, b) is that the signal amplitude started to decay despite ongoing stimulation. The signal maximum was observed typically 30 seconds after stimulation onset, thereafter the amplitude decreased significantly by 5 to 15 %. The fitted curves (Fig. 5a) were computed assuming single exponential signal build-up and decay with parameters described in the Materials and Method section. The exponentially decaying vasodilatory response of the neuronal signal is characterized by a time constant  $k_v = 0.02$  s<sup>-1</sup>. For the build-up of the BOLD signal the same initial rate  $k_{on} = 0.002$  s<sup>-1</sup> was assumed, irrespective of the stimulation amplitude applied. In contrast, the value for the decay rate constant  $k_{off}$  was found to decrease with increasing stimulation amplitude. This is also apparent when normalizing individual BOLD signals to the respective maximum intensity value (Fig 5b). Single exponential fitting for the averaged curves yielded first-order rate constants of  $k_{off}$  values of  $0.040$  s<sup>-1</sup> for 2.0 mA,  $0.051$  s<sup>-1</sup> for 1.5 mA and  $0.063$  s<sup>-1</sup> for 1.0 mA, displaying a linear dependence on the stimulation amplitude with a correlation factor of  $R^2 = 1.00$  (data not shown). In a next step we tested whether the decay rate  $k_{off}$  depended on the maximal BOLD change. We therefore used the average BOLD signals of all stimulation cycles (4 stimulation blocks per stimulation amplitude),

1  
2  
3  
4 which fulfilled the criteria with at least four data points exceeding the noise level used for the  
5  
6 fitting procedure (Fig. 5c): a significant negative correlation has been found with  $R^2 = 0.76$ .  
7  
8  
9

### 10 11 12 13 14 *Autoradiography and intrinsic optical measurements*

15  
16  
17 The autoradiography data of the two animals (Fig. 6b) showed a clear bilateral increase in FDG  
18  
19 uptake in the thalamus, consistent with the observed fMRI activation pattern (Fig. 6a). Cortical  
20  
21 activation was found to be weak. Bilateral local increases in cortical blood volume indicative of  
22  
23 neuronal activation were detected using intrinsic optical imaging (Fig 6d), which is in line with  
24  
25 our fMRI finding of bilateral cortical activation.  
26  
27  
28  
29  
30  
31  
32  
33

### 34 **Discussion**

35  
36  
37 fMRI in rodents, predominantly in rats, has become an important tool in biomedical research  
38  
39 e.g. to phenotype animal models of CNS disorders [36; 32; 37; 31]. In view of the many  
40  
41 genetically engineered mouse lines the development of robust procedures for mouse fMRI  
42  
43 protocols should be rewarding. By exploiting the significant gain in sensitivity provided by the  
44  
45 use of a cryogenic RF surface coil for signal detection [35; 3], BOLD fMRI data sets of high  
46  
47 quality suitable for reproducible quantitative analyses have been obtained. The CryoProbe  
48  
49 enabled fMRI at a spatial resolution of  $200 \times 200 \times 500 \mu\text{m}^3$ , which is sufficient to resolve the  
50  
51 major cerebral structures of the mouse brain and allows for detailed anatomical and functional  
52  
53 studies.  
54  
55  
56  
57  
58  
59

1  
2  
3  
4  
5  
6  
7  
8 The obtained fMRI data were highly reproducible both with regard to spatial extent and  
9  
10 temporal profile. This allowed reliable detection of even small changes in the BOLD amplitude  
11  
12 in response to stimulations at different current amplitudes. The BOLD intensity increased  
13  
14 significantly at each stimulus onset, though there was a net decrease of BOLD amplitude for  
15  
16 subsequent stimulation periods across the cycle consisting of four blocks. This was observed  
17  
18 before [18; 42] and might be due to adaptation or habituation mechanisms, occurring either  
19  
20 peripherally in the stimulated paw, or centrally in the brain. These mechanisms may also  
21  
22 contribute to the signal decrease observed during ongoing stimulation (Fig. 3a, b).  
23  
24  
25  
26  
27  
28

29 Due to the lack of clear evidence whether stimulation was noxious or not, the parameters used  
30  
31 were tested on a human subject under the presumption that the threshold to activate C- or A $\delta$ -  
32  
33 fibers is similar in humans and mice. However, as the innervation pattern differs, the human  
34  
35 values cannot be translated directly to the mouse but should rather be used as an estimate of  
36  
37 the noxious threshold. This stands in contrast to a study by Nair and Duong, which report hind  
38  
39 paw stimulation with amplitudes up to 7 mA to be somatosensory only [33]. To our experience,  
40  
41 the stimulation used in that study was likely to be noxious, at least at higher amplitudes.  
42  
43  
44  
45  
46  
47

48 Data analysis revealed a robust activation of the S1 cortical forelimb area. However, the signal  
49  
50 was not confined to the S1 region contralateral to the stimulated paw, but was also observed  
51  
52 on the ipsilateral side with essentially the same amplitude and spatial extent. This stands in  
53  
54 contrast to the majority of fMRI studies in healthy rats which report strictly unilateral responses  
55  
56 during unilateral electrical stimulation [53; 41; 15; 20] including our own study using isoflurane  
57  
58  
59

1  
2  
3  
4 anesthesia [48]. We performed additional experiments to modulate the laterality of the fMRI  
5  
6 response: varying anesthesia depths, male instead of female mice, or preparing only one paw  
7  
8 with electrodes to prevent possible crosstalk between the leads carrying the needle electrodes.  
9  
10 None of these interventions affected the bilateral symmetry of the activation pattern observed  
11  
12 (data not shown). In addition, electrical forepaw stimulation at 1.5 mA in another strain  
13  
14 (HsdWin:NMRI) showed the same bilateral activation pattern (data not shown). Bilateral  
15  
16 activation of the areas responsible for pain processing has also been observed in humans [45;  
17  
18 52; 47; 49; 46]. These bilateral signals may be conveyed by fibers of the corpus callosum [29] or  
19  
20 by commissural neurons of the spinal cord [38]. The occurrence of bilateral activation has also  
21  
22 been reported previously for rat studies [25]. However, due to our relatively slow temporal  
23  
24 resolution of 7.5 s, we were not able to resolve a possible delay between the onset of activation  
25  
26 in the two hemispheres. Even increasing the temporal resolution to 1 s was not sufficient to  
27  
28 reveal a potential delay of the ipsilateral versus the contralateral activation (data not shown).  
29  
30  
31  
32  
33  
34  
35  
36  
37  
38

39 Although carried out with a small number of animals, autoradiography and intrinsic optical  
40  
41 imaging experiments **support** our fMRI findings. Autoradiography revealed a distinct bilateral  
42  
43 activation of the thalamus, most pronounced in the ventral posterior nuclei, structures known  
44  
45 to relay nociceptive information. One mouse also showed bilateral cortical activation in the  
46  
47 regions of S2, insula and motor cortex. The intrinsic optical measurement showed a clear  
48  
49 bilateral activation of similar amplitudes in both hemispheres. These experiments, which were  
50  
51 performed independently from our fMRI setup, are in line with the results obtained with BOLD  
52  
53 fMRI.  
54  
55  
56  
57  
58  
59  
60  
61  
62  
63  
64  
65

1  
2  
3  
4 Besides the S1 region, bilateral activation was observed in the thalamus, the motor, S2 and  
5  
6 insular cortex. These regions are known to be part of the nociceptive network. Motor cortex  
7  
8 activation might originate from antidromic stimulation of the efferent motor fibers as seen in a  
9  
10 study by Cho and colleagues [9]. These activated areas are in accordance with those reported  
11  
12 for similar studies in rats [53].  
13  
14  
15  
16  
17

18 Anesthesia is a recurring issue in animal imaging, in particular when investigating nociception.  
19  
20 Isoflurane is an attractive anesthetic as it is easy to administer and control; however, there are  
21  
22 also drawbacks. Isoflurane is a potent vasodilator causing a global increase of cerebral blood  
23  
24 flow (CBF) in a dose dependent manner [27]. The basal energy level as derived from the  
25  
26 cerebral metabolic rate of glucose consumption ( $CMR_{glc}$ ) is lower than in the awake state. A  
27  
28 reduction by approximately 40% was reported for an isoflurane concentration of 1.4% [22]. In  
29  
30 comparison,  $\alpha$ -chloralose was found to reduce baseline  $CMR_{glc}$  by approximately 60% [25]. The  
31  
32 higher energy consumption, the high CBF and concomitantly the dilated vessels in isoflurane  
33  
34 anesthetized animals during baseline conditions reduce the dynamic range of the hemodynamic  
35  
36 response as compared to  $\alpha$ -chloralose anesthesia [10; 19]. The vasodilatory effects however  
37  
38 are dose dependent and can therefore be significantly reduced by using relatively low  
39  
40 isoflurane levels (at around 1%). At this low level we assume reduced antinociceptive efficacy of  
41  
42 isoflurane. Dedy et al. showed that the hypnotic effects of isoflurane occurred at lower  
43  
44 concentrations than the antinociceptive effects [12]. Also, low concentrations of isoflurane  
45  
46 appear to exhibit minimal neuro-suppressive effects, as the flow-metabolism coupling was  
47  
48 shown to remain preserved [16]. The robust BOLD response reported in this study as well as  
49  
50  
51  
52  
53  
54  
55  
56  
57  
58  
59  
60  
61  
62  
63  
64  
65

1  
2  
3  
4 data from other studies performed under isoflurane anesthesia prove it to be a useful  
5  
6  
7 anesthetic for fMRI studies in rodents [36; 32; 37; 40; 33; 43].  
8  
9

10 A recent study [1] performed on mice using electrical forepaw stimulation claims the  $\alpha$ 2-  
11  
12 adrenergic receptor agonist medetomidine to be better for long time studies than other  
13  
14 anesthetics. However, the occurrence of BOLD activation in less than 60% of all scans  
15  
16 performed (our study: > 95%) and the noisy temporal BOLD profiles do not clearly show the  
17  
18 superiority of medetomidine anesthesia.  
19  
20  
21  
22  
23

24 When analyzing the temporal BOLD profile, it became obvious that it consists of two  
25  
26 components, of which one is in phase with the stimulation (component *F*), while the other one  
27  
28 is much slower, starting with the onset of the first stimulation (component *S*). The two  
29  
30 components might be explained in terms of the underlying physiological processes: Component  
31  
32 *F* being in phase with the stimulation episodes, is probably associated with the peripheral  
33  
34 neuronal input of the A and C fibers, while the underlying signal described by component *S*  
35  
36 might reflect a slow vascular response.  
37  
38  
39  
40  
41  
42

43 The BOLD signal amplitude of both components depended linearly on the stimulation  
44  
45 amplitude. A similar linear dependence has been demonstrated using cerebral blood volume  
46  
47 (CBV) [31] and CBF [42] measurements in mice and rats, respectively. Torebjörk et al. also  
48  
49 showed that nociceptor responses and individual pain ratings in humans both linearly  
50  
51 correlated with the applied heat stimulation [51].  
52  
53  
54  
55  
56  
57  
58  
59  
60  
61  
62  
63  
64  
65

1  
2  
3  
4 By averaging and normalizing the BOLD signal curves of all animals, it became apparent that the  
5  
6 rate of the signal decay following a stimulation episode decreased with increasing stimulation  
7  
8 amplitudes. Stimulation at high amplitudes led to a larger BOLD response and thus to a higher  
9  
10 content of oxyhemoglobin (and correspondingly a lower concentration of deoxyhemoglobin) in  
11  
12 the vessels, as compared to stimulations at lower amplitudes. This is in line with the  
13  
14 hemodynamic model described by Friston and colleagues [14], which combines the balloon  
15  
16 model with a linear dynamic model of changes in CBF as caused by neuronal activity. The  
17  
18 balloon model describes the link between CBF and the BOLD signal and is able to predict  
19  
20 nonlinear effects of the BOLD signal, which contrast the linear relationship of CBF and synaptic  
21  
22 activity. The central concept of the model is to treat the venous compartment as an expandable  
23  
24 balloon, which is inflated by an increase in CBF, leading to a dilution of the deoxygenated blood  
25  
26 and an increased expelling rate of the blood [4]. The model predicts the recovery rate following  
27  
28 a stimulation episode to be proportional to the amount of deoxyhemoglobin in the vessel [5;  
29  
30 14; 4], which is in line with our experimental results (Fig.5). In contrast, the initial rate of the  
31  
32 build-up of the BOLD response was found independent on the current amplitude within error  
33  
34 limits.  
35  
36  
37  
38  
39  
40  
41  
42  
43  
44

45  
46 A further aspect that becomes apparent from the temporal profile of the BOLD response is that  
47  
48 the BOLD amplitude decays during stimulation despite ongoing peripheral input. This can be  
49  
50 explained by a decaying vasodilatory signal, which is also subject to feedback regulation by CBF,  
51  
52 in response to a prolonged neuronal stimulus [15, 45]. The neuronal input is described as an  
53  
54 initial peak followed by a decay to a lower level [14; 4].  
55  
56  
57  
58  
59



1  
2  
3  
4 We could demonstrate that reproducible mouse BOLD fMRI data can be obtained following  
5  
6  
7 sensory stimulation. The high quality of the data and the use of isoflurane make longitudinal  
8  
9  
10 studies to study e.g. functional changes in the brain feasible.  
11  
12  
13  
14  
15  
16  
17  
18  
19

## 20 **Acknowledgments**

21  
22  
23 The authors thank the NCCR Neural Plasticity and Repair and the Swiss National Science  
24  
25  
26 Foundation for funding this project. There are no conflicts of interest to declare.  
27  
28  
29  
30  
31

## 32 **References**

- 33  
34  
35  
36  
37 [1] Adamczak JM, Farr TD, Seehafer JU, Kalthoff D, Hoehn M. High field BOLD response to forepaw  
38  
39 stimulation in the mouse. *NeuroImage* 2010;51(2):704-712.  
40  
41 [2] Ahrens ET, Dubowitz DJ. Peripheral somatosensory fMRI in mouse at 11.7 T. *NMR in Biomedicine*  
42  
43 2001;14(5):318-324.  
44  
45 [3] Baltes C, Radzwill N, Bosshard S, Marek D, Rudin M. Micro MRI of the mouse brain using a novel 400  
46  
47 MHz cryogenic quadrature RF probe. *NMR Biomed* 2009;22(8):834-842.  
48  
49 [4] Buxton RB, Uludag K, Dubowitz DJ, Liu TT. Modeling the hemodynamic response to brain activation.  
50  
51 *NeuroImage* 2004;23 Suppl 1:S220-233.  
52  
53 [5] Buxton RB, Wong EC, Frank LR. Dynamics of blood flow and oxygenation changes during brain  
54  
55 activation: the balloon model. *Magn Reson Med* 1998;39(6):855-864.  
56  
57  
58  
59  
60  
61  
62  
63  
64  
65

- 1  
2  
3  
4 [6] Casey KL. Forebrain mechanisms of nociception and pain: analysis through imaging. Proc Natl Acad  
5  
6 Sci U S A 1999;96(14):7668-7674.  
7  
8
- 9 [7] Caterina MJ, Leffler A, Malmberg AB, Martin WJ, Trafton J, Petersen-Zeitl KR, Koltzenburg M,  
10  
11 Basbaum AI, Julius D. Impaired Nociception and Pain Sensation in Mice Lacking the Capsaicin  
12  
13 Receptor. Science 2000;288(5464):306-313.  
14  
15
- 16 [8] Chang C, Shyu B-C. A fMRI study of brain activations during non-noxious and noxious electrical  
17  
18 stimulation of the sciatic nerve of rats. Brain Research 2001;897(1-2):71-81.  
19  
20
- 21 [9] Cho YR, Pawela CP, Li R, Kao D, Schulte ML, Runquist ML, Yan JG, Matloub HS, Jaradeh SS, Hudetz AG,  
22  
23 Hyde JS. Refining the sensory and motor ratunculus of the rat upper extremity using fMRI and  
24  
25 direct nerve stimulation. Magn Reson Med 2007;58(5):901-909.  
26  
27
- 28 [10] Corfield DR, Murphy K, Josephs O, Adams L, Turner R. Does hypercapnia-induced cerebral  
29  
30 vasodilation modulate the hemodynamic response to neural activation? NeuroImage 2001;13(6  
31  
32 Pt 1):1207-1211.  
33  
34
- 35 [11] Davis KD, Taylor SJ, Crawley AP, Wood ML, Mikulis DJ. Functional MRI of pain- and attention-related  
36  
37 activations in the human cingulate cortex. J Neurophysiol 1997;77(6):3370-3380.  
38  
39
- 40 [12] Deady JE, Koblin DD, Eger EI, II, Heavner JE, D'Aoust B. Anesthetic Potencies and the Unitary Theory  
41  
42 of Narcosis. Anesth Analg 1981;60(6):380-384.  
43  
44
- 45 [13] Franklin K, Paxinos G. The Mouse Brain in Stereotaxic Coordinates. San Diego: Academic Press,  
46  
47 1997.  
48
- 49 [14] Friston KJ, Mechelli A, Turner R, Price CJ. Nonlinear Responses in fMRI: The Balloon Model, Volterra  
50  
51 Kernels, and Other Hemodynamics. NeuroImage 2000;12(4):466-477.  
52  
53
- 54 [15] Goloshevsky AG, Silva AC, Dodd SJ, Koretsky AP. BOLD fMRI and somatosensory evoked potentials  
55  
56 are well correlated over a broad range of frequency content of somatosensory stimulation of  
57  
58 the rat forepaw. Brain Research 2008;1195:67-76.  
59  
60

- 1  
2  
3  
4 [16] Hansen TD, Warner DS, Todd MM, Vust LJ. The role of cerebral metabolism in determining the local  
5  
6 cerebral blood flow effects of volatile anesthetics: evidence for persistent flow-metabolism  
7  
8 coupling. *J Cereb Blood Flow Metab* 1989;9(3):323-328.  
9
- 10  
11 [17] Harvey RJ, Depner UB, Wassle H, Ahmadi S, Heindl C, Reinold H, Smart TG, Harvey K, Schutz B, Abo-  
12  
13 Salem OM, Zimmer A, Poisbeau P, Welzl H, Wolfer DP, Betz H, Zeilhofer HU, Muller U. GlyR  
14  
15 {alpha}3: An Essential Target for Spinal PGE2-Mediated Inflammatory Pain Sensitization. *Science*  
16  
17 2004;304(5672):884-887.  
18  
19
- 20  
21 [18] Hsu EW, Hedlund LW, MacFall JR. Functional MRI of the rat somatosensory cortex: Effects of  
22  
23 hyperventilation. *Magnetic Resonance in Medicine* 1998;40(3):421-426.  
24
- 25  
26 [19] Kemna LJ, Posse S. Effect of respiratory CO(2) changes on the temporal dynamics of the  
27  
28 hemodynamic response in functional MR imaging. *NeuroImage* 2001;14(3):642-649.  
29
- 30  
31 [20] Kida I, Yamamoto T. Stimulus frequency dependence of blood oxygenation level-dependent  
32  
33 functional magnetic resonance imaging signals in the somatosensory cortex of rats. *Neurosci Res*  
34  
35 2008;62(1):25-31.  
36
- 37  
38 [21] Ledent C, Valverde O, Cossu G, Petitet F, ccedil, ois, Aubert J-F, Beslot F, oise, ouml, hme GA,  
39  
40 Imperato A, Pedrazzini T, Roques BP, Vassart G, Fratta W, Parmentier M. Unresponsiveness to  
41  
42 Cannabinoids and Reduced Addictive Effects of Opiates in CB1 Receptor Knockout Mice. *Science*  
43  
44 1999;283(5400):401-404.  
45  
46
- 47 [22] Lenz C, Rebel A, van Ackern K, Kuschinsky W, Waschke KF. Local Cerebral Blood Flow, Local Cerebral  
48  
49 Glucose Utilization, and Flow-Metabolism Coupling during Sevoflurane versus Isoflurane  
50  
51 Anesthesia in Rats. *Anesthesiology* 1998;89(6):1480-1488.  
52  
53
- 54 [23] Lilja J, Endo T, Hofstetter C, Westman E, Young J, Olson L, Spenger C. Blood Oxygenation Level-  
55  
56 Dependent Visualization of Synaptic Relay Stations of Sensory Pathways along the Neuroaxis in  
57  
58 Response to Graded Sensory Stimulation of a Limb. *J Neurosci* 2006;26(23):6330-6336.  
59  
60

- 1  
2  
3  
4 [24] Linden Avd, Camp Nv, Ramos-Cabrer P, Hoehn M. Current status of functional MRI on small animals:  
5  
6 application to physiology, pathophysiology, and cognition. *NMR Biomed* 2007;20(5):522-545.  
7  
8  
9 [25] Maandag NJ, Coman D, Sanganahalli BG, Herman P, Smith AJ, Blumenfeld H, Shulman RG, Hyder F.  
10  
11 Energetics of neuronal signaling and fMRI activity. *Proc Natl Acad Sci U S A* 2007;104(51):20546-  
12  
13 20551.  
14  
15  
16 [26] Manning BH, Morgan MJ, Franklin KB. Morphine analgesia in the formalin test: evidence for  
17  
18 forebrain and midbrain sites of action. *Neuroscience* 1994;63(1):289-294.  
19  
20  
21 [27] Matta BF, Heath KJ, Tipping K, Summors AC. Direct cerebral vasodilatory effects of sevoflurane and  
22  
23 isoflurane. *Anesthesiology* 1999;91(3):677-680.  
24  
25  
26 [28] Millan MJ. The induction of pain: an integrative review. *Progress in Neurobiology* 1999;57(1):1-164.  
27  
28 [29] Mohajerani MH, McVea DA, Fingas M, Murphy TH. Mirrored Bilateral Slow-Wave Cortical Activity  
29  
30 within Local Circuits Revealed by Fast Bihemispheric Voltage-Sensitive Dye Imaging in  
31  
32 Anesthetized and Awake Mice. *J Neurosci*;30(10):3745-3751.  
33  
34  
35 [30] Morrow TJ, Paulson PE, Danneman PJ, Casey KL. Regional changes in forebrain activation during the  
36  
37 early and late phase of formalin nociception: analysis using cerebral blood flow in the rat. *Pain*  
38  
39 1998;75(2-3):355-365.  
40  
41  
42 [31] Mueggler T, Baumann D, Rausch M, Staufenbiel M, Rudin M. Age-Dependent Impairment of  
43  
44 Somatosensory Response in the Amyloid Precursor Protein 23 Transgenic Mouse Model of  
45  
46 Alzheimer's Disease. *J Neurosci* 2003;23(23):8231-8236.  
47  
48  
49 [32] Mueggler T, Sturchler-Pierrat C, Baumann D, Rausch M, Staufenbiel M, Rudin M. Compromised  
50  
51 hemodynamic response in amyloid precursor protein transgenic mice. *J Neurosci*  
52  
53 2002;22(16):7218-7224.  
54  
55  
56 [33] Nair G, Duong TQ. Echo-planar BOLD fMRI of mice on a narrow-bore 9.4 T magnet. *Magn Reson*  
57  
58 *Med* 2004;52(2):430-434.  
59  
60  
61  
62  
63  
64  
65

- 1  
2  
3  
4 [34] Nassar MA, Stirling LC, Forlani G, Baker MD, Matthews EA, Dickenson AH, Wood JN. Nociceptor-  
5  
6 specific gene deletion reveals a major role for Nav1.7 (PN1) in acute and inflammatory pain.  
7  
8 Proc Natl Acad Sci U S A 2004;101(34):12706-12711.  
9
- 10  
11 [35] Ratering D, Baltés C, Nordmeyer-Massner J, Marek D, Rudin M. Performance of a 200-MHz  
12  
13 cryogenic RF probe designed for MRI and MRS of the murine brain. Magn Reson Med  
14  
15 2008;59(6):1440-1447.  
16  
17
- 18 [36] Reese T, Bjelke B, Porszasz R, Baumann D, Bochelen D, Sauter A, Rudin M. Regional brain activation  
19  
20 by bicuculline visualized by functional magnetic resonance imaging. Time-resolved assessment  
21  
22 of bicuculline-induced changes in local cerebral blood volume using an intravascular contrast  
23  
24 agent. NMR Biomed 2000;13(1):43-49.  
25  
26
- 27 [37] Reese T, Bochelen D, Baumann D, Rausch M, Sauter A, Rudin M. Impaired functionality of  
28  
29 reperfused brain tissue following short transient focal ischemia in rats. Magn Reson Imaging  
30  
31 2002;20(6):447-454.  
32  
33
- 34 [38] Ruscheweyh R, Sandkühler J. Long-range oscillatory Ca<sup>2+</sup> waves in rat spinal dorsal  
35  
36 horn. European Journal of Neuroscience 2005;22(8):1967-1976.  
37  
38
- 39 [39] Sanganahalli BG, Bailey CJ, Herman P, Hyder F. Tactile and non-tactile sensory paradigms for fMRI  
40  
41 and neurophysiologic studies in rodents. Methods Mol Biol 2009;489:213-242.  
42  
43
- 44 [40] Sauter A, Reese T, Porszasz R, Baumann D, Rausch M, Rudin M. Recovery of function in  
45  
46 cytoprotected cerebral cortex in rat stroke model assessed by functional MRI. Magn Reson Med  
47  
48 2002;47(4):759-765.  
49  
50
- 51 [41] Silva AC, Koretsky AP, Duyn JH. Functional MRI impulse response for BOLD and CBV contrast in rat  
52  
53 somatosensory cortex. Magn Reson Med 2007;57(6):1110-1118.  
54  
55  
56  
57  
58  
59  
60  
61  
62  
63  
64  
65

- 1  
2  
3  
4 [42] Silva AC, Lee SP, Yang G, Iadecola C, Kim SG. Simultaneous blood oxygenation level-dependent and  
5  
6 cerebral blood flow functional magnetic resonance imaging during forepaw stimulation in the  
7  
8 rat. *J Cereb Blood Flow Metab* 1999;19(8):871-879.  
9
- 10 [43] Sommers MG, Egmond Jv, Booij LH, Heerschap A. Isoflurane anesthesia is a valuable alternative for  
11  
12  $\alpha$ -chloralose anesthesia in the forepaw stimulation model in rats. *NMR in*  
13  
14 *Biomedicine* 2009;22(4):414-418.  
15  
16
- 17 [44] Spaeth N, Wyss MT, Weber B, Scheidegger S, Lutz A, Verwey J, Radovanovic I, Pahnke J, Wild D,  
18  
19 Westera G, Weishaupt D, Hermann DM, Kaser-Hotz B, Aguzzi A, Buck A. Uptake of 18F-  
20  
21 Fluorocholine, 18F-Fluoroethyl-L-Tyrosine, and 18F-FDG in Acute Cerebral Radiation Injury in the  
22  
23 Rat: Implications for Separation of Radiation Necrosis from Tumor Recurrence. *J Nucl Med*  
24  
25 2004;45(11):1931-1938.  
26  
27  
28  
29
- 30 [45] Stancák A, Svoboda J, Rachmanová R, Vrána J, Králík J, Tintera J. Desynchronization of cortical  
31  
32 rhythms following cutaneous stimulation: effects of stimulus repetition and intensity, and of the  
33  
34 size of corpus callosum. *Clinical Neurophysiology* 2003;114(10):1936-1947.  
35  
36
- 37 [46] Staud R, Craggs JG, Robinson ME, Perlstein WM, Price DD. Brain activity related to temporal  
38  
39 summation of C-fiber evoked pain. *Pain* 2007;129(1-2):130-142.  
40  
41
- 42 [47] Sutherland MT, Tang AC. Reliable detection of bilateral activation in human primary somatosensory  
43  
44 cortex by unilateral median nerve stimulation. *NeuroImage* 2006;33(4):1042-1054.  
45  
46
- 47 [48] Sydekum E, Baltés C, Ghosh A, Mueggler T, Schwab ME, Rudin M. Functional reorganization in rat  
48  
49 somatosensory cortex assessed by fMRI: elastic image registration based on structural  
50  
51 landmarks in fMRI images and application to spinal cord injured rats. *NeuroImage*  
52  
53 2009;44(4):1345-1354.  
54  
55
- 56 [49] Terekhin P, Forster C. Hypocapnia related changes in pain-induced brain activation as measured by  
57  
58 functional MRI. *Neuroscience Letters* 2006;400(1-2):110-114.  
59  
60  
61  
62  
63  
64  
65

1  
2  
3  
4  
5  
6  
7  
8  
9  
10  
11  
12  
13  
14  
15  
16  
17  
18  
19  
20  
21  
22  
23  
24  
25  
26  
27  
28  
29  
30  
31  
32  
33  
34  
35  
36  
37  
38  
39  
40  
41  
42  
43  
44  
45  
46  
47  
48  
49  
50  
51  
52  
53  
54  
55  
56  
57  
58  
59  
60  
61  
62  
63  
64  
65

[50] Thal SC, Plesnila N. Non-invasive intraoperative monitoring of blood pressure and arterial pCO<sub>2</sub> during surgical anesthesia in mice. *Journal of Neuroscience Methods* 2007;159(2):261-267.

[51] Torebjork HE, LaMotte RH, Robinson CJ. Peripheral neural correlates of magnitude of cutaneous pain and hyperalgesia: simultaneous recordings in humans of sensory judgments of pain and evoked responses in nociceptors with C-fibers. *J Neurophysiol* 1984;51(2):325-339.

[52] Torquati K, Pizzella V, Babiloni C, Gratta CD, Penna SD, Ferretti A, Franciotti R, Rossini PM, Romani GL. Nociceptive and non-nociceptive sub-regions in the human secondary somatosensory cortex: An MEG study using fMRI constraints. *NeuroImage* 2005;26(1):48-56.

[53] Tuor UI, Malisza K, Foniok T, Papadimitropoulos R, Jarmasz M, Somorjai R, Kozlowski P. Functional magnetic resonance imaging in rats subjected to intense electrical and noxious chemical stimulation of the forepaw. *Pain* 2000;87(3):315-324.

[54] Wilson SG, Mogil JS. Measuring pain in the (knockout) mouse: big challenges in a small mammal. *Behav Brain Res* 2001;125(1-2):65-73.

[55] Wyss MT, Obrist NM, Haiss F, Eckert R, Stanley R, Burger C, Buck A, Weber B. A beta-scintillator for surface measurements of radiotracer kinetics in the intact rodent cortex. *NeuroImage* 2009;48(2):339-347.

1  
2  
3  
4 **Figure Captions**  
5  
6  
7

8 **Figure 1:** Spatial distribution of the BOLD activation. **(a)** Sagittal reference image indicating the  
9 positions of the coronal EPI slices covering a large section of the mouse forebrain. **(b) – (f)**  
10 Spatial distribution of the activated clusters ( $p = 0.0001$ ) of one representative animal after  
11 unilateral forepaw stimulation. The left side of the image corresponds to the left hemisphere.  
12 Nominal distance to the interaural line (IAL) is given for each slice. Scale bar indicates 5 mm.  
13 Activated areas include the S1 forelimb area **(c, d, e)**; motor cortex M1 **(c, d, e)**; and several  
14 nuclei of the thalamus, including the ventral posterior nucleus which relays somatosensory  
15 information **(f)**. Activated clusters are also observed at the sagittal sinus **(e, f)**. **(g)** Time course  
16 of the BOLD signal after unilateral electrical stimulation of the forepaw at 1.5 mA for S1  
17 contralateral to the stimulated paw (pink), S1 ipsilateral (dashed black), thalamus (gray), and  
18 the control region (light gray). Gray bars indicate the stimulation periods. The BOLD signals of  
19 the contralateral and ipsilateral S1 are almost identical. **(h)** Maximal signal amplitude of  
20 different regions (S1, S2, insular cortex (IC), piriform cortex (PC, control region)) ipsi- (black  
21 circles) and contralateral (pink squares) to the stimulated paw at 1.5 mA. All values are given as  
22 mean + SEM. **(i)** Activation map of two representative animals showing activation of the  
23 forepaw (blue) and hind paw (red) S1 area after stimulation of the respective paw at 1.5 mA,  
24 overlaid on an EPI image. Scale bars indicate t-values.  
25  
26  
27  
28  
29  
30  
31  
32  
33  
34  
35  
36  
37  
38  
39  
40  
41  
42  
43  
44  
45  
46  
47  
48  
49  
50  
51  
52  
53  
54  
55

56 **Figure 2:** Activation maps of the cortex after left and right forepaw stimulation at **(a,g)** 0.5 mA,  
57 **(b,h)** 1.0 mA, **(c,i)** 1.5 mA, **(d,j)** 2.0 mA. Data show activated clusters derived from GLM analysis  
58  
59



1  
2  
3  
4 (p = 0.0001, cluster size: 15 voxels) for all animals overlaid on the mouse brain atlas at IAL +3.7  
5  
6  
7 mm **(a-f)** and IAL +2.8 mm **(g-l)** [13]. **(e-k)** Mouse brain atlas with relevant regions (SI: primary  
8  
9 somatosensory cortex, forepaw region; SII: secondary somatosensory cortex; IC: insular cortex;  
10  
11 MI: primary motor cortex; TN: thalamic nuclei) overlaid on the anatomical image. **(f,l)**  
12  
13 Representative EPI image revealing relatively little distortions. **(g-j)** Activation maps; intensity  
14  
15 indicates the number of stimulation periods displaying significant BOLD activation at a given  
16  
17 location (scale bar).  
18  
19  
20  
21  
22  
23  
24  
25  
26

27 **Figure 3: (a)** Relative change of the BOLD signal intensity as a function of time during electrical  
28  
29 forepaw stimulation for the different stimulation amplitudes. Dark grey bars indicate the  
30  
31 stimulation periods, light gray boxes mark data points used for fitting the component *S* curve  
32  
33  
34 **(b).** **(c)** Signal component *F* obtained by subtracting **(b)** from **(a)**. Values are given as mean +  
35  
36 SEM.  
37  
38  
39  
40  
41  
42  
43

44 **Figure 4:** The amplitudes of the two components *S* **(a)** and *F* **(b)** as a function of the stimulation  
45  
46 amplitude. **(a)** Linear regression analysis yielded correlation factors of  $R^2 = 0.98$  for the  
47  
48 contralateral and  $R^2 = 0.97$  for the ipsilateral S1 somatosensory cortical area. The corresponding  
49  
50 value for thalamus was  $R^2 = 0.81$ . **(b)** For the fast component the correlation factors were:  $R^2 =$   
51  
52  $0.97$  for contralateral S1,  $R^2 = 0.98$  for ipsilateral S1 and  $R^2 = 0.87$  for thalamus. Values are given  
53  
54 as mean  $\pm$  SEM.  
55  
56  
57  
58  
59  
60  
61  
62  
63  
64  
65

1  
2  
3  
4  
5  
6  
7  
8 **Figure 5:** Analysis of component  $F$  of the fMRI response to electrical stimulation of the forepaw  
9  
10 in the contralateral S1 cortical region. **(a)** Mean fMRI signal response for the first stimulation  
11 episode as a function of time and current amplitude. Solid lines indicate the BOLD response  
12 modeled as described in the text. The dashed line illustrates the vasodilatory stimulus, which  
13 displays a single exponential decay with a rate constant  $k_v = 0.02 \text{ s}^{-1}$ . **(b)** The mean normalized  
14 fMRI response of the first stimulation period (normalized to 1) as a function of time and  
15 stimulation amplitude. The reduced rate of signal decay with increasing stimulus amplitude  
16 (and correspondingly higher maximum BOLD intensity) becomes apparent. For sake of clarity  
17 error bars have been omitted. **(c)** The decay rate constant of the BOLD signal of the single  
18 animals decrease with increasing maximal intensity of the BOLD signal. Linear regression  
19 yielded a correlation coefficient of  $R^2 = 0.76$ . Values are given as mean  $\pm$  SEM.  
20  
21  
22  
23  
24  
25  
26  
27  
28  
29  
30  
31  
32  
33  
34  
35  
36  
37  
38  
39  
40

41 **Figure 6:** Autoradiography and intrinsic optical imaging. **(a)** fMRI activation map of a  
42 representative animal. **(b)**  $^{18}\text{F}$ -FDG autoradiographies of two mice after unilateral forepaw  
43 stimulation show bilateral thalamic activation and some bilateral cortical activation (blue  
44 arrows). **(c)** Reflection of 570 nm light used for intrinsic optical imaging reveals the vascular  
45 anatomy at both sides of the sagittal sinus. **(d)** Activation map of intrinsic optical imaging shows  
46 bilateral activation of the somatosensory area. Regions with increased cerebral blood volume  
47 are recognized by a decrease in signal intensity (blue). Color bar indicates changes in signal  
48 intensity in [%].  
49  
50  
51  
52  
53  
54  
55  
56  
57  
58  
59  
60  
61  
62  
63  
64  
65

## \*Summary

1  
2  
3  
4  
5  
6  
7  
8  
9  
10  
11  
12  
13  
14  
15  
16  
17  
18  
19  
20  
21  
22  
23  
24  
25  
26  
27  
28  
29  
30  
31  
32  
33  
34  
35  
36  
37  
38  
39  
40  
41  
42  
43  
44  
45  
46  
47  
48  
49  
50  
51  
52  
53  
54  
55  
56  
57  
58  
59  
60  
61  
62  
63  
64  
65

### Summary

The development of a robust BOLD fMRI protocol using electrical forepaw stimulation allowed studying somatosensory and nociceptive processing in mice.

Figure 1  
[Click here to download high resolution image](#)

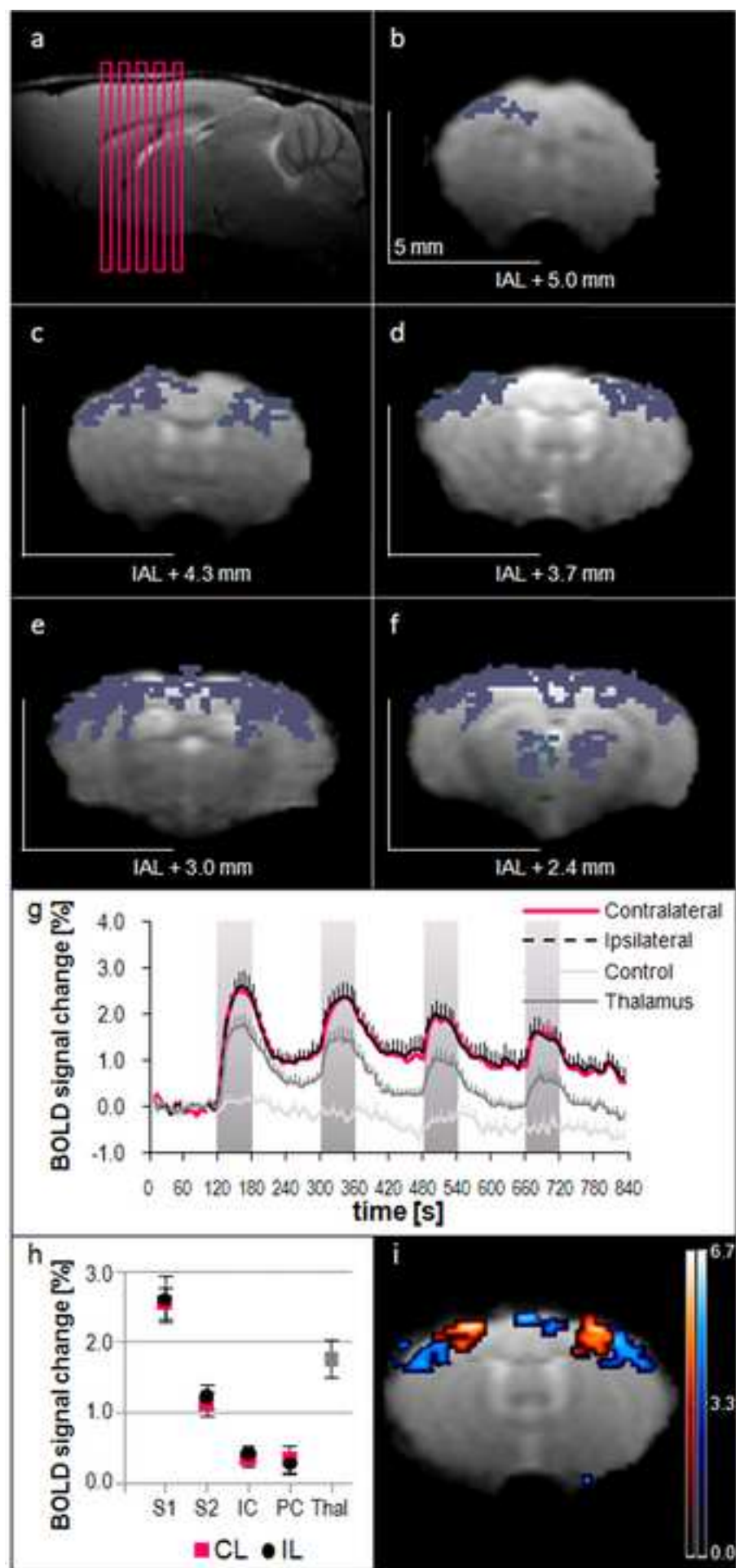


Figure 2  
[Click here to download high resolution image](#)

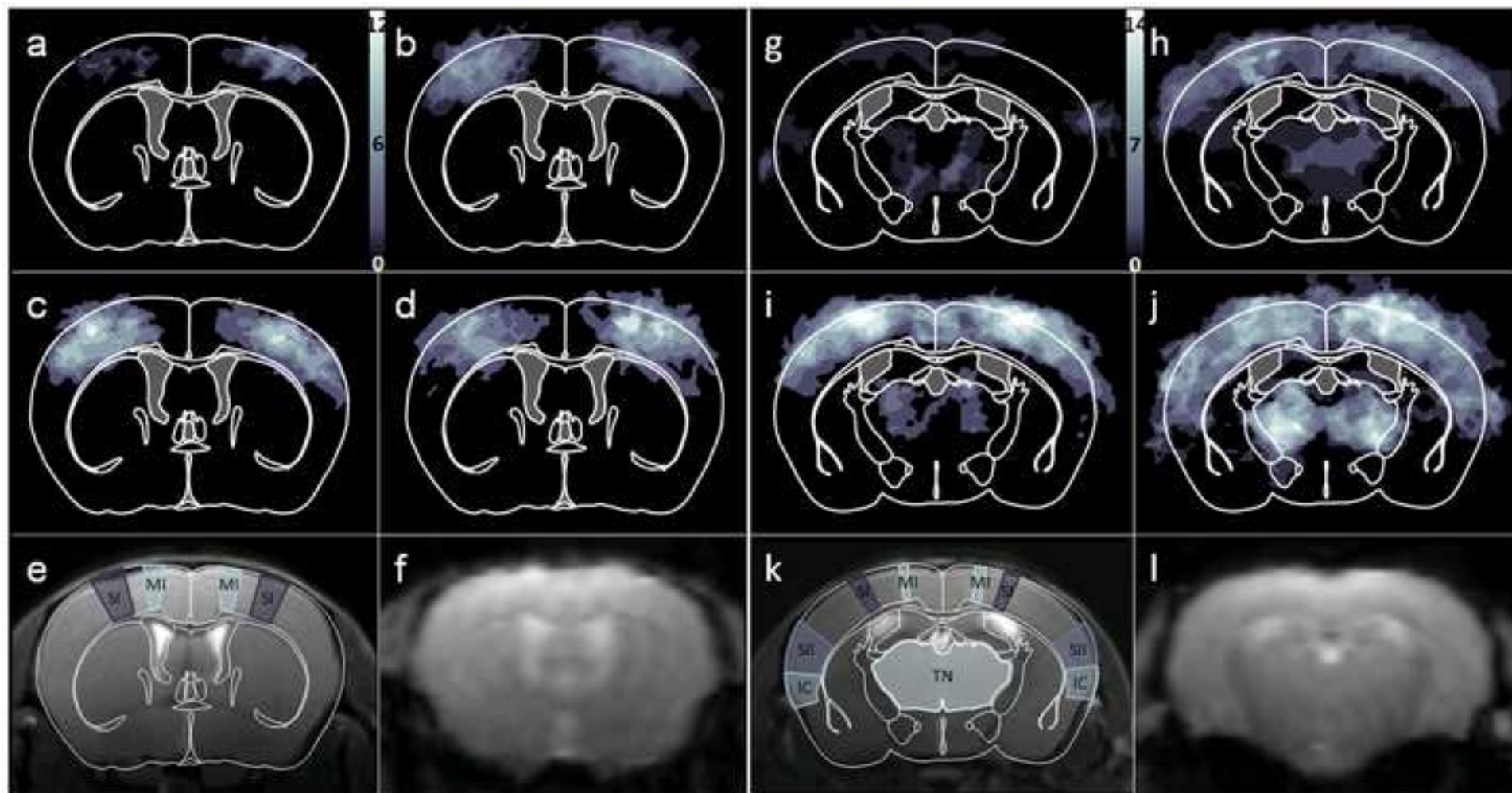


Figure 3  
[Click here to download high resolution image](#)

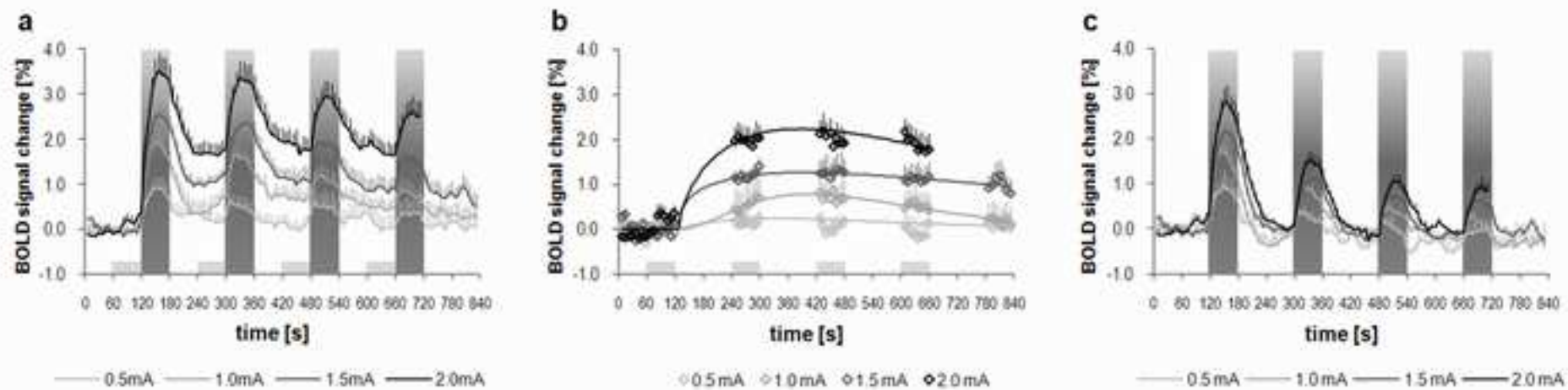


Figure 4  
[Click here to download high resolution image](#)

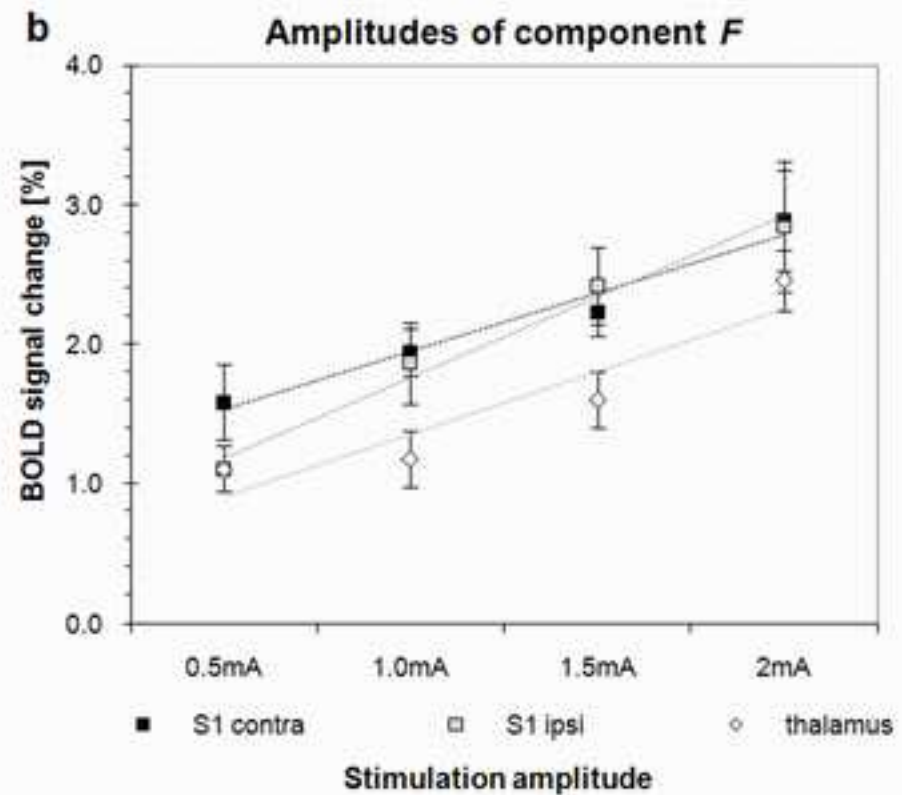
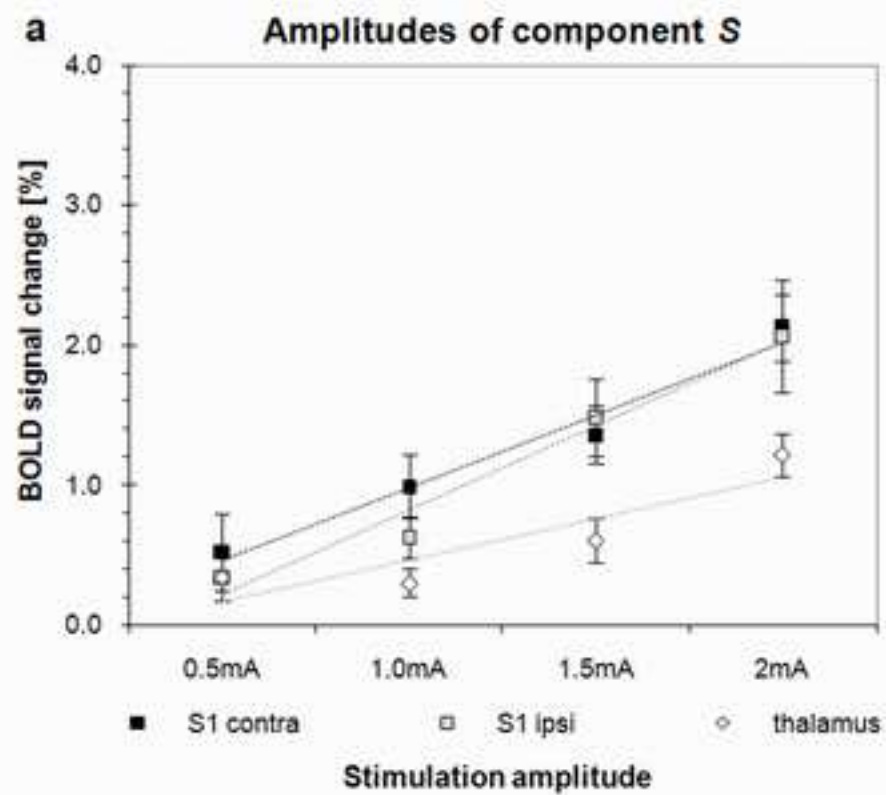


Figure 5  
[Click here to download high resolution image](#)

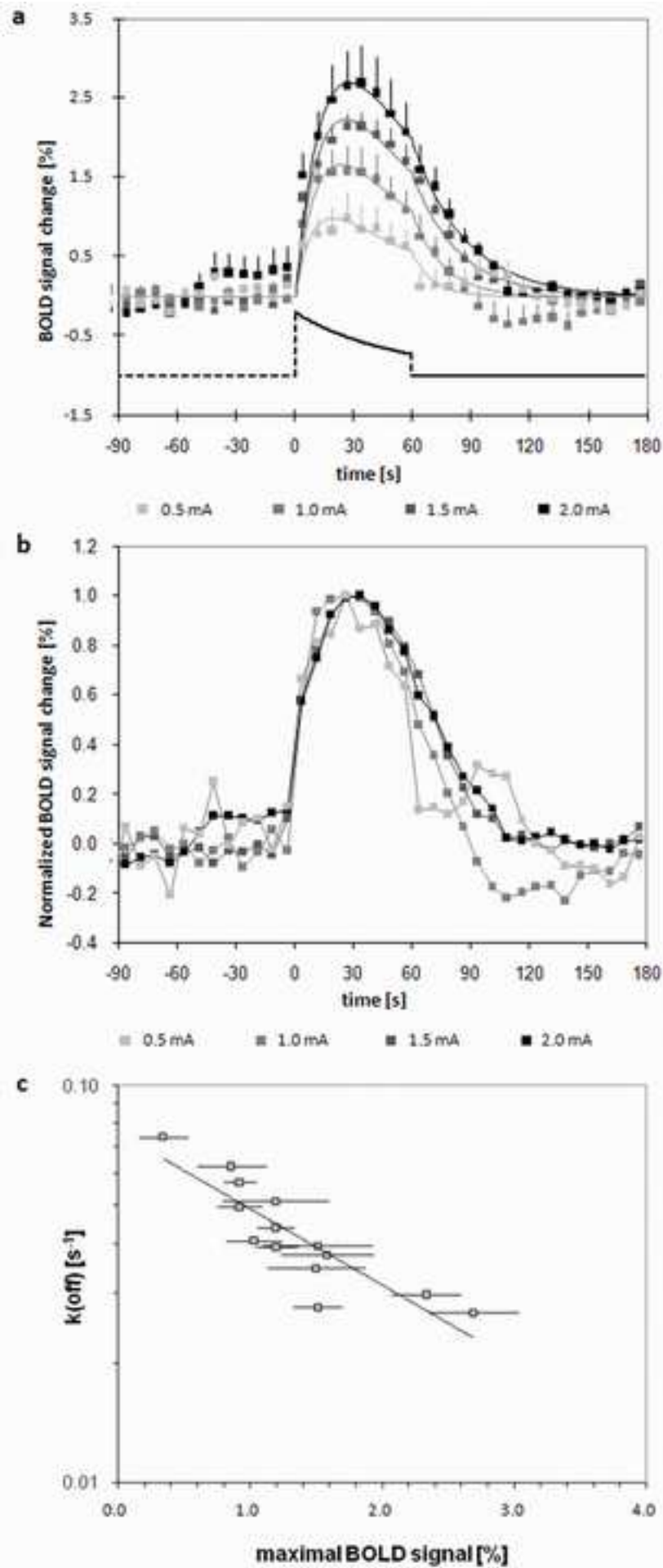




Figure 6  
[Click here to download high resolution image](#)

